

Received: 2018.04.16  
Accepted: 2018.05.06  
Published: 2018.09.14

# Time-Course Investigation of Intervertebral Disc Degeneration Induced by Different Sizes of Needle Punctures in Rat Tail Disc

Authors' Contribution:  
Study Design A  
Data Collection B  
Statistical Analysis C  
Data Interpretation D  
Manuscript Preparation E  
Literature Search F  
Funds Collection G

BCDE 1,2 **Tao Chen**  
ABCF 3 **Xiaofei Cheng**  
ACG 2 **Jingcheng Wang**  
ACD 2 **Xinmin Feng**  
AG 2 **Liang Zhang**

1 Xiangya School of Medicine, Central South University, Changsha, Hunan, P.R. China  
2 Department of Orthopedics, Clinical Medical College of Yangzhou University, Yangzhou, Jiangsu, P.R. China  
3 Department of Orthopedic Surgery, Shanghai Ninth People's Hospital, Shanghai Jiao Tong University School of Medicine, Shanghai, P.R. China

**Corresponding Author:** Liang Zhang, e-mail: zhangliang6320@sina.com

**Source of support:** This work was supported by the National Natural Science Foundation for Young Scholars of China (no. 81401830) and the Young Medical Scholars Major Program of Jiangsu Province (No. QNRC2016342)

**Background:** This study aimed to determine the best size needle to use in inducing IVDD and to find the proper time point of disc degeneration suitable for further biologic treatment study.

**Material/Methods:** First, rat tail level 5/6, 7/8, and 9/10 discs were punctured by 18G, 21G, or 25G needles. Then, degeneration was assessed by radiography, MRI, and histological evaluation at 2, 4, and 6 weeks after puncture. Later, real-time reverse transcriptase (RT-PCR) was used to examine mRNA expressions of aggrecan, collagen type II, hypoxia-inducible factor-1 $\alpha$  (HIF-1 $\alpha$ ), glucose transporter1 (GLUT-1), and vascular endothelial growth factor (VEGF).

**Results:** Significant differences were identified in almost all parameters compared with the control group in the 18G and 21G group at almost all time points. To assess the effect of different needle sizes on DHI, we used magnetic resonance imaging (MRI), grade, and mRNA expression. We found significant differences between different groups, except for DHI between the 21G group and 25G group and MRI grade between the 18G and 21G group at the 2-week time point. In assessing the effect of different needle sizes on HE staining score and toluidine blue staining grade, statistical differences were observed at some time points. The effects of time on all parameters were significant at almost all time points in all groups.

**Conclusions:** The middle-size needle (21G) performed better in inducing disc degeneration. The 2-week time point may be better for use in further experimental studies.

**MeSH Keywords:** Hypoxia-Inducible Factor 1, alpha Subunit • Intervertebral Disc Degeneration • Models, Animal • Needles • Punctures

**Full-text PDF:** <https://www.medscimonit.com/abstract/index/idArt/910636>

 3549  1  7  36



## Background

Low back pain (LBP) is one of the most common and costly public health problems in many countries today, both in terms of huge medical care costs and disability of afflicted individuals [1,2]. It is reported that this disease affects 40% of the U.S. adult population at some stage in their life and accounts for over \$100 billion annually in medical cost and disability [3]. Despite the prevalence of LBP, clear understanding of the pathophysiology and pathogenesis remains poorly understood. Intervertebral disc degeneration (IVDD) is generally well accepted to be the most crucial and strongly associated with LBP and is characterized by dysfunctional cells followed by loss of proteoglycan production [4–6]. Despite its high prevalence, current treatments options, including medications, physical therapy, epidural injections and invasive-surgical intervention, only alleviate symptoms instead of reversing degeneration [5,7].

With recent progress in molecular biology and biomaterials, numerous biological therapies to repair or regenerate degenerated intervertebral disc (IVD) have been advocated [5,8,9]. Although the experimental results of such strategies are encouraging [8,9], the shift to clinical application requires further evaluation of the safety and effectiveness. Thus, an *in vivo* simple and reproducible IVDD model is essential for the transition from scientific concepts to clinical applications.

Although a variety of IVDD animal models have been developed, each with its own advantages and disadvantages [7,10–13], no practical and easily reproducible model currently exists. An ideal animal model must be ethical, uncomplicated, reproducible, controllable, clinically relevant to the human situation, and cost-effective. The annulus needle puncture is the most frequently used disc injury method as it directly alters mechanical properties via nucleus pulposus (NP) depressurization, while also minimizing annulus fibrosus (AF) damage. Recently, the rat tail disc has been proposed as a readily accessible platform for the needle puncture model of inducing IVDD [13–21] because the rat tail disc has a convenient anatomic location and can be manipulated easily, requiring only minor surgery. The rat tail disc is also comparable mechanically to the human lumbar disc and has wide commercial availability of biological assays [22–24].

Although the use of needle puncture has gained popularity, we still feel that previous studies have not addressed some important issues. A needle diameter to disc height ratio of 40% is required to cause changes in lumbar disc mechanics [25]. The disc degeneration is dependent on the needle size as well as the elapsed time following the puncture. When considering the appropriate needle size, Han et al. used a 20-G needle in tail disc 7/8 [14], Zhang et al. used an 18G or 21G needle in tail disc 5/6 or 7/8 [13], and Keorochana et al. used 18G, 20G, and

22G needles in tail disc 6/7 or 8/9 [15]. However, no such has focussed on determining the best size needle to use for puncture to induce IVDD. Standardization of the IVDD model is essential to target different stages of degeneration, as it is believed that severity of degeneration can influence the potential therapeutic effect.

In this study, we investigated the best size needle to use for puncture to induce IVDD and assessed the proper time point of disc degeneration best suited for further study of the effect of biologic treatment.

## Material and Methods

### Animals, reagents, and materials

Thirty-six Sprague-Dawley rats (weight, 300–400 g; age, 4–6 months) were purchased from the Laboratory Animal Center of Jiangsu University (License No. SCXK (Su) 2013-0011). The animal experiments conformed to the Guide for the Care and Use of Laboratory Animals published by the US National Institutes of Health and were approved by the Institutional Review Board of the Clinical Medical College of Yangzhou University, Yangzhou, China. Animals were bred in a natural ventilated room, with 12-h light/dark cycle, a temperature of 25–28°C, and a relative humidity of 70–85%.

### Surgical procedure

The surgical procedure was performed as previously described [13]. Briefly, anesthesia was achieved by 3.6% chloral hydrate (10 ml/kg) injected into the abdominal cavity and maintained by inhalation of anesthetic isoflurane. Rats were placed in prone position and the tail skin disinfected with povidone-iodine solution. Under fluoroscopic guidance, a percutaneous needle puncture with 18G, 21G, and 25G needles (HuaYi Bio-technology, Shanghai, China) was performed in 3 intervals levels: coccygeal (Co) 5-6, Co7-8, and Co9-10. The Co6-7 and Co8-9 served as intact controls. The needle was carefully inserted in the middle of the disc, perpendicular to the skin and parallel to the endplates, rotated 180°, and held for 5 s. After removal of the needle, the wound was covered with gauze and the rat underwent the standard postoperative procedures.

### Radiographic analysis

Lateral plane radiographs were taken before puncture and at each time point thereafter (2, 4, and 6 weeks) using the same anesthesia method as indicated above. The animal was placed in the prone position with tail straight, which created the vertical beam to the tail and focus at the target levels with a Faxitron MX-20 digital cabinet X-ray system (Faxitron

X-ray Corporation, USA). Lateral plane images were obtained using the following settings: distance 6.50 inches, exposure 20 s, and penetration power 60 kV. Two independent observers who were blinded to the different needle sizes and follow-up periods performed the radiographic assessment. IVD heights were measured and expressed as disc height index (DHI) according to the method described by Han et al. [14]. Additionally, DHI change expressed as %DHI was calculated using the following formula:

$$\%DHI = (\text{post-punctured DHI} / \text{pre-punctured DHI}) \times 100\%$$

### Magnetic resonance imaging (MRI) analysis

Immediately after the radiography, MRI was performed to estimate the signal and structural changes in T2-weighted sagittal images at each follow-up time point using a 7.0 T animal-specific MRI system (Bruker Pharmascan, Germany). T2-weighted sections of the median sagittal plane were obtained using the following settings: a fast spin echo (SE) sequence with a TR (time to repetition) of 3000 ms and a TE (time to echo) of 70 ms; the slice thickness was 0.5 mm with a 0 mm gap; and number of averages, 2. MRI were evaluated based on changes in the degree and area of signal intensity from 1 (normal) to 4 (severe decrease of signal intensity) using the modified Pfirrmann classification [26].

### Histological analysis

The intact IVDs with adjacent vertebral bodies were harvested for histological analysis immediately after euthanasia. The specimens were fixed in 4% paraformaldehyde for 24 h and then decalcified in 10% EDTA for 7 days. After being embedded in paraffin, the specimens were sectioned to a thickness of 5  $\mu\text{m}$  for hematoxylin and eosin (HE) and toluidine blue staining. The histological sections were evaluated by 2 blinded observers. The HE staining score and toluidine blue staining grade were graded according to the criteria of Keorochana [15].

### Real-time reverse transcriptase (RT-PCR)

Total RNA was extracted IVDs using Trizol reagent following the manufacturer's instructions. RNA quality and quantity were determined by measuring the optical density at a 260-nm (OD260) wavelength using a spectrophotometer. Then, the cDNA of total RNA was obtained using a reverse-transcribed reagent (Takara, Japan). RT-PCR was performed to analyze mRNA expressions of collagen type II, aggrecan, hypoxia-inducible factor-1 $\alpha$  (HIF-1 $\alpha$ ), glucose transporter1 (GLUT-1), vascular endothelial growth factor (VEGF), and glyceraldehyde 3-phosphate dehydrogenase (GAPDH). The cycling conditions were initial denaturation at 95°C for 20 s, followed by 40 cycles at 95°C for 5 s, primer annealing at 60°C for 20 s, and elongation at 72°C for 15 s. The  $\Delta\text{Ct}$  was calculated by subtracting the Ct for GAPDH from

**Table 1.** Description of the designed primers.

Gene	Forward and reverse primers and enzyme sites	Fragment length, bp
Col II	5'AAGAAGCACATCTGGTTTGA3'	121
	5'CAGTGGACAGTAGACGGAGGA3'	
Aggrecan	5'GGTGGTACCCACATCGC3'	149
	5'GCTGGCTCCATTAGTCT3'	
HIF-1 $\alpha$	5'GTCTCCATTACCTGCCTCTG3'	296
	5'GATTCTTCGCTTCTGTCTTC3'	
VEGF	5'ACCCACAAGAGCTAGATAG3'	299
	5'CCTCTTCACTAAATGACAGTCCC3'	
GLUT-1	5'ATCAAACATGGAACCACCGTAT3'	201
	5'AACCATAAGCACGGCAGAC3'	
GAPDH	5'TGACTTCAACAGCGACCCCA3'	121
	5'CACCCTGTTGCTGTAGCCAAA3'	

Col II – collagen type II; HIF-1 $\alpha$  – hypoxia inducible factor-1 $\alpha$ ; VEGF – vascular endothelial growth factor; GLUT-1 – glucose transporter1; GAPDH – glyceraldehyde-3-phosphate dehydrogenase.

the Ct for each target gene, where Ct is the cycle threshold. The  $\Delta\text{Ct}$  for each treated group was further normalized to the intact control group to obtain  $\Delta\Delta\text{Ct}$ . Relative expression was calculated using the  $2^{-\Delta\Delta\text{Ct}}$  method. Primers for RT-PCR were designed and synthesized by Invitrogen (Carlsbad, CA) (Table 1).

### Statistical analysis

All statistical analyses were performed using SPSS Statistics 20.0 software (IBM, USA). All data are presented as the mean  $\pm$  standard deviation. The paired-samples *t* test was used to detect significant differences between the punctured disc and the control disc. One-way analysis of variance (ANOVA) was performed for the effect of needle sizes and time period after puncture on DHI% and gene expression. Nonparametric data (histological grade and MRI grade) were analyzed by use of Mann-Whitney U tests. *P*-values less than 0.05 were considered statistically significant.

## Results

### Radiographic assessment

Figure 1 shows representative radiographs of the rat tail discs punctured by different size needles obtained at different

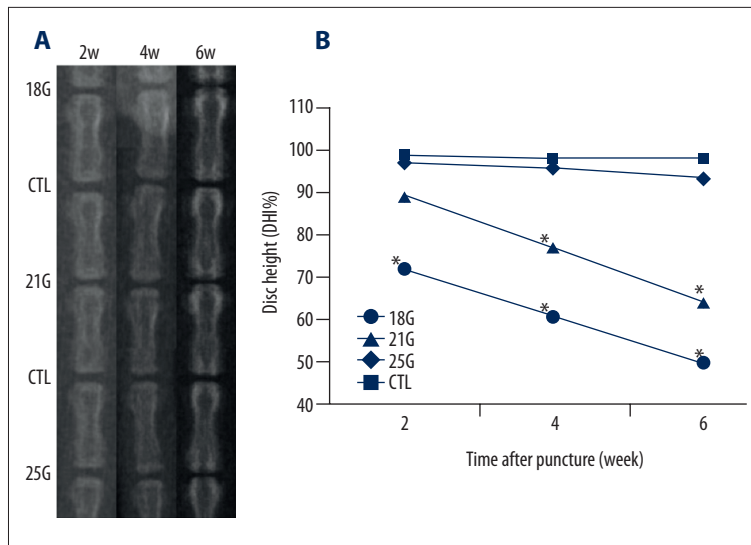


**Figure 1.** (A) Representative X-ray images of rat tail punctured by needles of all sizes, obtained at different time points. (B) The disc heights began to decrease in the 18G group from 2-week time point and 21G group from 4-week time point. CTL – control; DHI – disc height index. \* Compared with control.

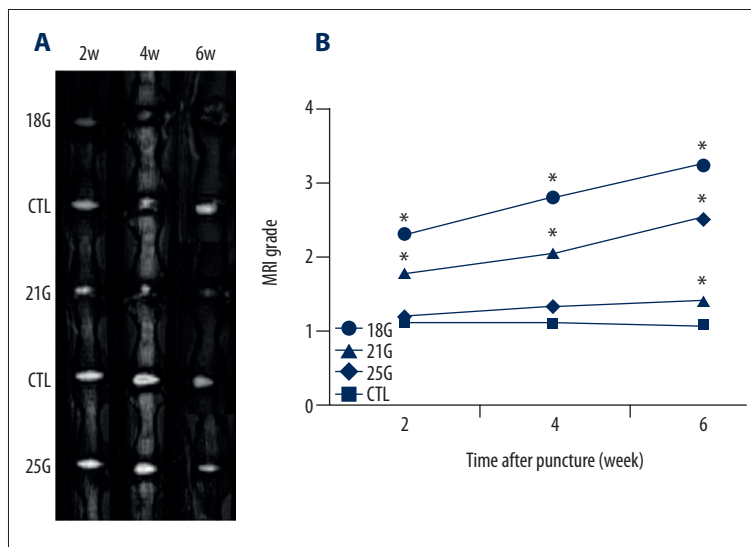


**Figure 2.** (A) Representative MRI images of rat tail punctured by all needle sizes obtained at different time points. (B) The MRI grade began to increase in the 18G and 21G group from 2-week time point. CTL – control; MRI – magnetic resonance imaging. \* Compared with control group.

time points. The disc height, indicated as%DHI, began to decrease in the 18G group from 2-week time point and 21G group from 4-week time point, and the decrease continued throughout the experimental period (all  $P < 0.05$ ). There were no significant differences in DHI% between the control group and 25G group over a 6-week period. For the effect of different needle sizes on%DHI, significant differences were found between different groups at all time points post-puncture (all  $P < 0.05$ ), except between 21G and 25G groups at 2-week time point. The effect of time to DHI was significant at all time points in the 18G and 21G groups, and between 2-week and 4-week time points in the 25G group (all  $P < 0.05$ ) (Figure 1B).

### MRI assessment

MRI images revealed the changes in signal intensity and structures of the discs punctured by at different time points

(Figure 2A). The disc MRI grade of the punctured disc compared with the control disc, 18G, and 21G groups had significantly more degeneration after puncture (all  $P < 0.05$ ). Significant MRI change in the 25G group was observed only at 6-week time point after puncture ( $P < 0.05$ ). For the effect of different needle sizes on MRI grade, we observed significant differences between the 18G and 21G groups at 4-week and 6-week time points (both  $P < 0.05$ ). At all time points after puncture, significant differences were observed between the 18G and 25G groups (all  $P < 0.05$ ) and between the 21G and 25G groups (all  $P < 0.05$ ). The effect of time to MRI grade after different size needle punctures was significant at all time points, except between 2-week and 4-week time points and between 4-week and 6-week time points in the 25G group ( $P < 0.05$ ) (Figure 2B).

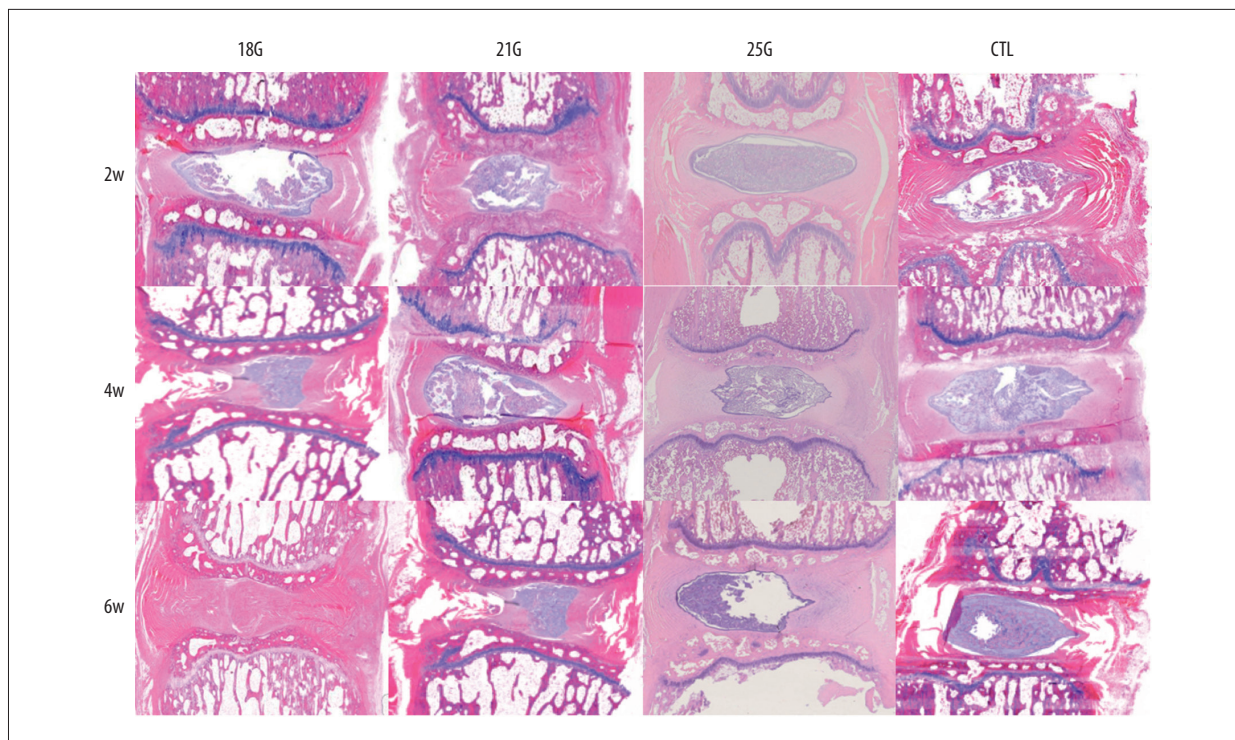


**Figure 3.** HE staining sections of the rat tail discs punctured by all sizes of needles, obtained at different time points. The control group exhibited intact AF, rounded NP and well-defined border between them, whereas the punctured discs exhibited disordered AF, fewer NP cells, and with an interrupted border (HE, 40 $\times$ ). CTL – control.

### Histological analysis

The histologic appearances of degenerated discs were markedly affected by puncture needle size. Rat tail disc sections exhibited diverse morphologies, from normal to severely degenerated (Figure 3). The control group exhibited intact AF, rounded NP, and well-defined borders between them, whereas the punctured discs exhibited disordered AF, fewer NP cells, and an interrupted border. HE staining score demonstrated significant differences between the control group and the 18G and 21G group at all time points after puncture (all  $P < 0.05$ ), and 25G only at 6-week time point ( $P < 0.05$ ). The effect of needle size on HE staining score was assessed; there were significant differences between 18G and 21G (both  $P < 0.05$ ), 21G and 25G groups (both  $P < 0.05$ ) at 4-week and 6-week time points. Significant differences were also identified between 18G and 25G groups at all time points after puncture (all  $P < 0.05$ ). Significant changes in HE staining score with different size needles with respect to time were seen at all time points (all  $P < 0.05$ ), except between 2-week and 4-week time points in the 21G group and between 2-week and 4-week time points, and between 4-week and 6-week time points in the 25G group (Figure 4A).

The control group exhibited NP chondrocytes and positive proteoglycan staining, whereas the punctured discs demonstrated fewer NP chondrocytes and a reduction in the intensity of

staining. As shown in Figure 4B and Figure 5, toluidine blue staining grades of the punctured discs were significantly different when compared with the control group over a 6-week period (all  $P < 0.05$ ). The size of the needle affected the toluidine blue staining, with a statistically significant difference between the 18G and 21G group only at the 6-week time point ( $P < 0.05$ ), between 21G and 25G at the 4-week time point ( $P < 0.05$ ), and between the 18G and 25G groups at 4-week and 6-week time points (both  $P < 0.05$ ). Significant differences were only found between 2-week and 6-week time points in the 18G and 21G groups (both  $P < 0.05$ ) with respect to time.

### Gene expression

The mRNA expressions of aggrecan and collagen type II increased temporarily at 2-week time point and decreased gradually over time in the 25G group, whereas expressions of aggrecan and collagen type II progressively decreased over time in the 18G and 21G groups (all  $P < 0.05$ ) (Figure 6). The genetic expressions of HIF-1 $\alpha$ , GLUT-1, and VEGF progressively increased after puncture over time in all groups (all  $P < 0.05$ ) (Figure 7). The effect of different needle sizes on the mRNA expression levels of aggrecan, collagen type II, HIF-1 $\alpha$ , GLUT-1, and VEGF were also evaluated, showing significant differences between all groups at all time points (all  $P < 0.05$ ). The effect of time on mRNA expression levels of aggrecan, collagen type II, HIF-1 $\alpha$ ,

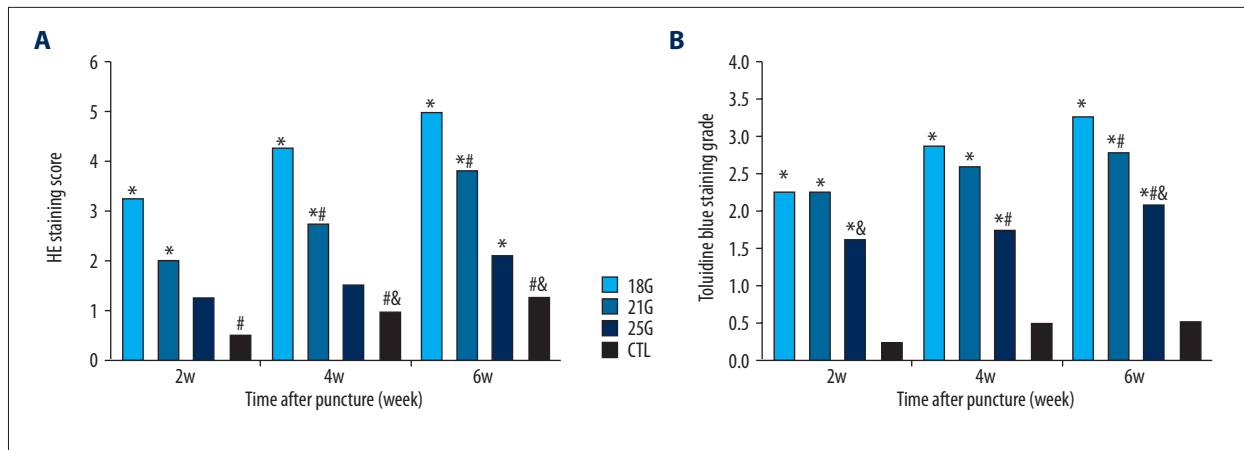


**Figure 4.** (A) HE staining score of the rat tail discs punctured by all sizes of needles, obtained at different time points. (B) Toluidine blue staining grade of the rat tail discs punctured by all sizes of needles, obtained at different time points. CTL – control. \* Compared with control group; # compared with 18G group; & compared with 21G group.

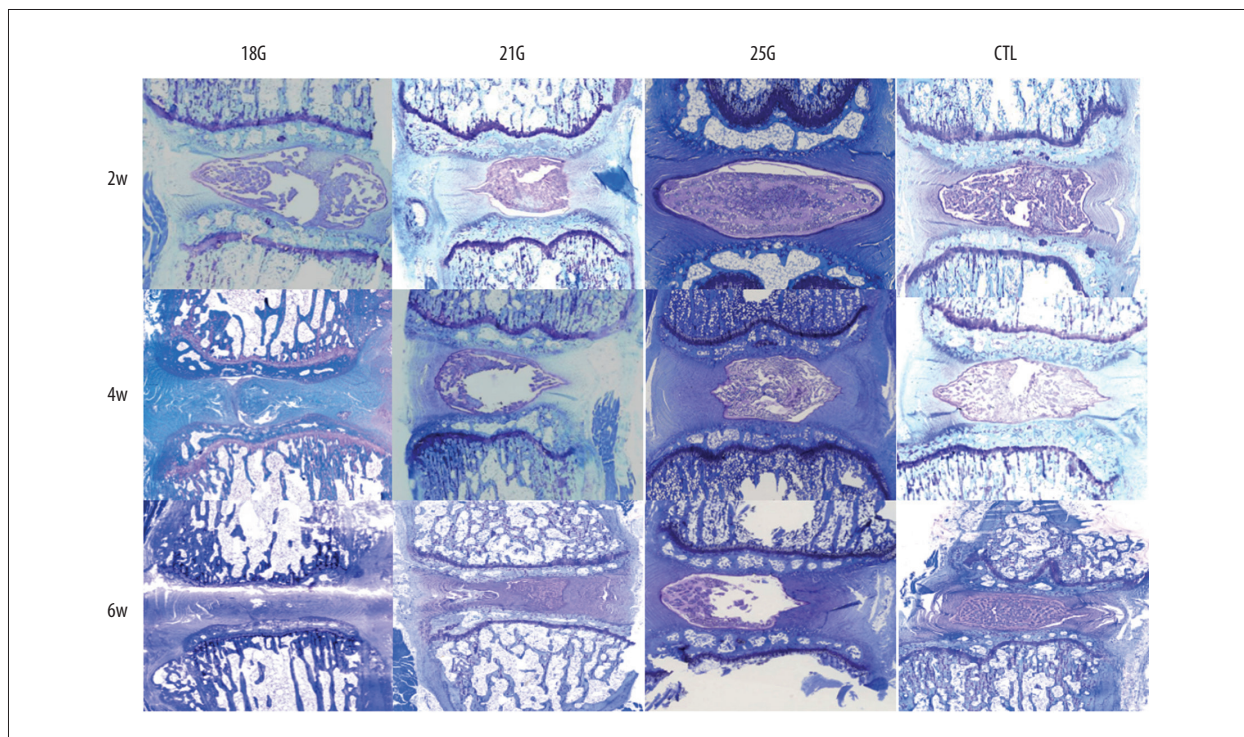


**Figure 5.** Toluidine blue staining sections of the rat tail discs punctured by all sizes of needles, obtained at different time points. The control group exhibited NP chondrocytes and positive proteoglycan staining, whereas the punctured discs demonstrated fewer NP chondrocytes and a reduction in the intensity of staining (Toluidine blue, 40×). CTL – control.

GLUT-1, and VEGF after different size needle punctures were significant at all time points in all groups (all  $P < 0.05$ ).

## Discussion

### The feasibility of rat tail disc for inducing IVDD

Preclinical disease animal models remain an important step in the translational development of novel biomedical technologies. The needle puncture model of IVDD is widely used and slowly yields progressive, mild, reproducible degeneration

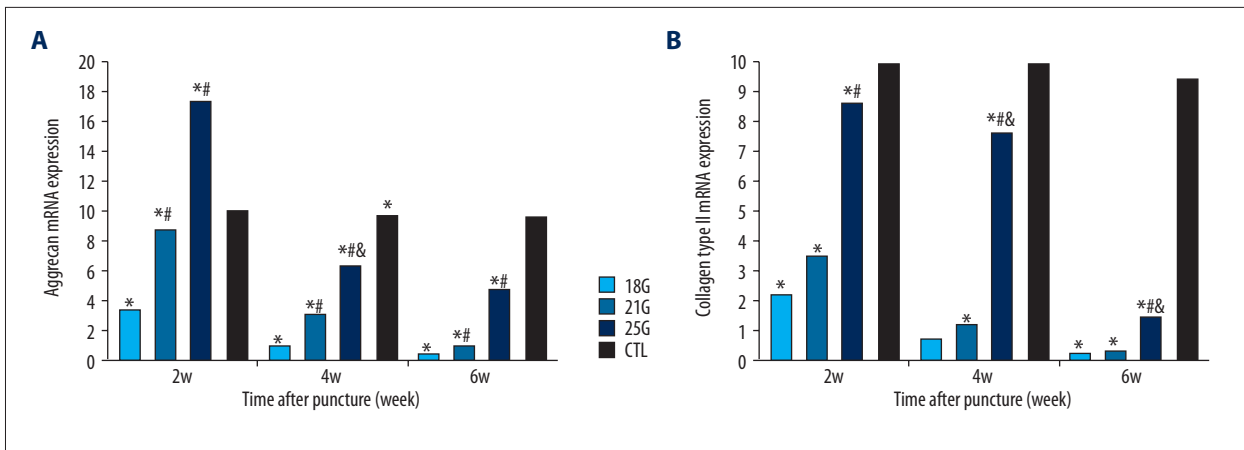


**Figure 6.** The relative mRNA expressions of aggrecan and collagen type II of the rat tail discs punctured by all sizes of needles, obtained at different time points. (A) Aggrecan relative expression. (B) Collagen type II relative expression. CTL – control. \* Compared with control group; # compared with 18G group; & compared with 21G group.

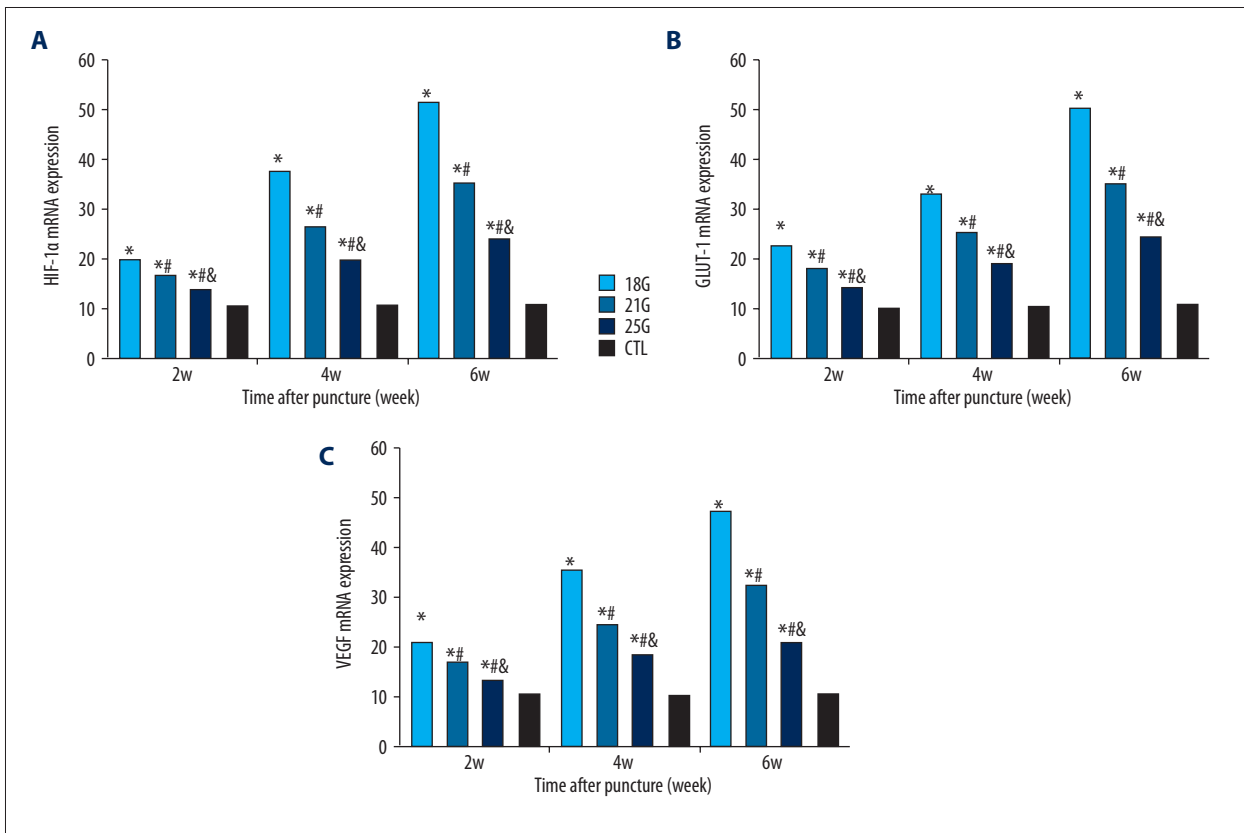


**Figure 7.** The relative mRNA expressions of HIF-1α, GLUT-1 and VEGF of the rat tail discs punctured by all sizes of needles, obtained at different time points. (A) HIF-1α relative expression. (B) GLUT-1 relative expression. (C) GLUT-1 relative expression. CTL – control; HIF-1α – hypoxia-inducible factor-1α; GLUT-1 – glucose transporter1; VEGF – vascular endothelial growth factor. \* Compared with control group; # compared with 18G group; & compared with 21G group.

pathological and biochemical changes that mimic human IVDD [15–21]. These degeneration changes of the disc were induced through AF tear with NP leakage. The animals most commonly used as *in vivo* models are mice, rats, rabbits, dogs,

goats, and pigs [27–30]. Although the higher species have more cellular components similar to humans, the higher cost and difficult availability are the primary concerns. The rat tail disc has been proposed as a platform for the puncture model not

only because it is a low-cost, simple, efficient, reproducible, and less invasive technique [13,20,25,27], but also because it has the same geometry, mechanical properties, proteoglycan, and collagen content as the human disc [22–24]. Our results show that percutaneous needle puncture of the rat tail IVD can induce slow, progressive radiographic, histologic, and biochemical degeneration, as revealed by X-ray, MRI, histology, and RT-PCR, which were similar to the degenerative changes in human IVDD, suggesting that the rat tail can be used as a reliable animal model for IVDD.

### The effect of the needle size on the degree of degeneration

The injury severity of induced IVDD caused by needle puncture affects the subsequent rate of degeneration. The injury severity of IVDD is directly correlated to the size of the needle and the puncture depth used. The injury caused by the needle puncture should be large enough to disrupt biomechanical function to drive degenerative changes in the rat tail disc AF. Various sizes of needles (18G–30G) have been chosen to induce IVDD, as reported before [13–21,28,31]. However, there is no standardized method in terms of the effect of the injury severity, which is important for the effect of biologic therapy in different stages of degeneration. Many studies confirmed that the ratio of needle diameter to disc height is the key parameter to initiate disc changes [25]. Zhang et al. investigated the effect of different needle sizes (18G and 21G, 100% and 51% ratio of diameter to disc height) on biomechanical and histological changes in rat tail discs. The results showed that all punctured discs can develop disc degeneration according to MRI images and histological outcome measurements [13]. Keorochana et al. performed a needle puncture with 18G, 20G, and 22G size needles (100%, 60%, and 48% ratio of diameter to disc height) in the rat tail disc model [15]. The results showed larger needle gauges produce more degenerative discs, as shown by radiography, MRI, and immunohistochemistry. Chen et al. punctured rat tail discs using 0.8-mm diameter Kirschner needles (85% ratio of diameter to disc height) and the result demonstrated the degenerative changes were similar to human IVDD [20]. However, the best needle size for the rat tail disc puncture to induce IVDD is still unknown.

In the present study, with 18G, 21G, and 25G needle sizes and the ratio of needle inside diameter to disc height at 100%, 51%, and 27%, respectively, we found that larger needle size creates more degenerative changes with time, especially when comparing the 18G and 25G groups. According to the results of RT-PCR, the mRNA expression of aggrecan and collagen type II showed a slow decline in the 21G group, and even a temporarily increase in the 25G group at the 2-week time point, suggesting a certain degree of repair activity in the early stage of IVDD. However, the 18G group demonstrated

narrower disc height and higher histology scores (more serious degenerative) than that of the 21G and 25G groups at all time points after puncture, suggesting that 21G is the best size needle to use in puncturing rat tail discs to induce stable and reliable IVDD model.

### The effect of time after puncture on the degree of degeneration

The main purpose of establishment of IVDD animal models is to investigate the feasibility of the mechanism and new treatment of IVDD. It is generally believed that biological treatment should begin in the early stage. The major components of the extracellular matrix are proteoglycans and collagen type II in NP. The progression of IVDD is associated with a significant decrease in the levels of proteoglycans and collagen type II of NP. A study that investigated the long-term progression of IVDD induced by 21G needle puncture in rat tail disc model confirmed a transient up-regulation in the gene expression of aggrecan and collagen type II. After 10–17 days, these chondrocytic gene markers decreased and returned to control levels [17]. Another study revealed that gene expression of collagen type II increased at 3 days postoperatively and declined gradually over time in the 21G needle puncture rat tail disc model [20].

In the present study, gene expressions of aggrecan and collagen type II declined slowly at the 2-week time point owing to the endogenous repair ability of the injured NP, and then decreased in the 21G group. There was a statistically significant difference in gene expression levels between the 21G group and all other groups at 2-week time point, suggesting the degeneration degree was not very serious and that the degenerated NP still had rich collagen type II and proteoglycan expression. DHI% in the 21G group declined at 2-week time point after surgery, although without a significant difference compared with that of the control group. However, the 21G group had significantly more degeneration degree when compared with the control group at 2-week time point using MRI grade. The histological analysis also confirmed that the IVD degenerated at 2-week time point. Combined information from DHI and MRI T2 images construct a set of novel biomarkers that could be used to identify degenerating discs that are approaching the threshold [32]. It is believed that biological treatments should be indicated in mild to moderate stage of IVDD, as sufficient NP cells are needed for these treatments to be effective [33]. Thus, the 2-week time point may be the threshold time point to receive biological treatment to reverse the degenerated change of the IVD.

### The possible mechanism of IVDD and the role of HIF-1 $\alpha$

IVD is the largest avascular structure, characterized by low oxygen tension *in vivo*. HIF is a master transcription factor that

regulates the expression of a number of genes involved in glycolysis as well as mitochondrial energy metabolism in responses to hypoxic environments. HIF plays an important role in the regulation of matrix production, metabolism, apoptosis, and autophagy of NP cells in the process of IVDD [34]. HIF-1 $\alpha$  has been recently demonstrated in normal and herniated human NP tissue [35]. HIF-1 $\alpha$  maintains the metabolic activities of NP cells under a hypoxic environment in IVD via the regulation of GLUT expression, which is one of the important genes involved in promoting anaerobic glycolysis of NP cells in hypoxia responsiveness [36]. HIF-1 $\alpha$  is also a potent regulatory factor of VEGF, which is the key protein in both physiological and pathological angiogenesis. By transactivating glycolysis-related genes such as GLUT-1 and GLUT-3, the oxemic-independent stabilization of HIF-1 $\alpha$  is presumed to give NP cells metabolic adaptations to the deficiency of oxygen and nutrition. The expression of HIF-1 $\alpha$  and GLUT-1 in the degenerative NP was higher than that in the normal NP [34]. In the present study, the expressions of HIF-1 $\alpha$ , VEGF, and GLUT-1 increased over time after puncture, suggesting that HIF-1 $\alpha$  can induce the expression of VEGF and GLUT-1 in the progression of IVDD. Thus, HIF-1 $\alpha$  may be a potential target for the prevention and treatment of IVDD.

## References:

- Hoy D, March L, Brooks P et al: The global burden of low back pain: Estimates from the Global Burden of Disease 2010 study. *Ann Rheum Dis*, 2014; 73: 968–74
- Hoy D, Brooks P, Blyth F et al: The epidemiology of low back pain. *Best Pract Res Clin rheumatol*, 2010; 24: 769–81
- Katz JN: Lumbar disc disorders and low-back pain: Socioeconomic factors and consequences. *J Bone Joint Surg Am*, 2006; 88(Suppl. 2): 21–24
- Zheng CJ, Chen J: Disc degeneration implies low back pain. *Theor Biol Med Model*, 2015; 12: 24
- Weber KT, Jacobsen TD, Maidhof R et al: Developments in intervertebral disc disease research: Pathophysiology, mechanobiology, and therapeutics. *Curr Rev Musculoskelet Med*, 2015; 8: 18–31
- Luoma K, Riihimäki H, Luukkainen R et al: Low back pain in relation to lumbar disc degeneration. *Spine*, 2000; 25: 487–92
- Than KD, Rahman SU, Wang L et al: Intradiscal injection of simvastatin results in radiologic, histologic, and genetic evidence of disc regeneration in a rat model of degenerative disc disease. *Spine J*, 2014; 14: 1017–28
- Wang Z, Perez-Terzic CM, Smith J et al: Efficacy of intervertebral disc regeneration with stem cells – A systematic review and meta-analysis of animal controlled trials. *Gene*, 2015; 564: 1–8
- Yim RL-H, Lee JT-Y, Bow CH et al: A systematic review of the safety and efficacy of mesenchymal stem cells for disc degeneration: Insights and future directions for regenerative therapeutics. *Stem Cells Dev*, 2014; 23: 2553–67
- Sakai D, Nishimura K, Tanaka M et al: Migration of bone marrow-derived cells for endogenous repair in a new tail-looping disc degeneration model in the mouse: A pilot study. *Spine J*, 2015; 15: 1356–65
- Li D, Yang H, Huang Y et al: Lumbar intervertebral disc puncture under C-arm fluoroscopy: A new rat model of lumbar intervertebral disc degeneration. *Exp Anim*, 2014; 63: 227–34
- Issy AC, Castania V, Castania M et al: Experimental model of intervertebral disc degeneration by needle puncture in Wistar rats. *Braz J Med Biol Res*, 2013; 46: 235–44
- Zhang H, La Marca F, Hollister SJ et al: Developing consistently reproducible intervertebral disc degeneration at rat tail spine by using needle puncture. *J Neurosurg Spine*, 2009; 10: 522–30
- Han B, Zhu K, Li FC et al: A simple disc degeneration model induced by percutaneous needle puncture in the rat tail. *Spine*, 2008; 33: 1925–34
- Keorochana G, Johnson JS, Taghavi CE et al: The effect of needle size inducing degeneration in the rat tail disc: Evaluation using radiograph, magnetic resonance imaging, histology, and immunohistochemistry. *Spine J*, 2010; 10: 1014–23
- Michalek AJ, Funabashi KL, Iatridis JC: Needle puncture injury of the rat intervertebral disc affects torsional and compressive biomechanics differently. *Eur Spine J*, 2010; 19: 2110–16
- Zhang H, Yang S, Wang L et al: Time course investigation of intervertebral disc degeneration produced by needle-stab injury of the rat tail spine: Laboratory investigation. *J Neurosurg Spine*, 2011; 15: 404–13
- Martin JT, Gorth DJ, Beattie EE et al: Needle puncture injury causes acute and long-term mechanical deficiency in a mouse model of intervertebral disc degeneration. *J Orthop Res*, 2013; 31: 1276–82
- Li D, Yang H, Huang Y et al: Lumbar intervertebral disc puncture under C-arm fluoroscopy: A new rat model of lumbar intervertebral disc degeneration. *Exp Anim*, 2014; 63: 227–34
- Chen CH, Chiang CJ, Wu LC et al: Time course investigation of intervertebral disc degeneration in a rat-tail puncture model. *Life Sci*, 2016; 156: 15–20
- Cunha C, Lamas S, Gonçalves RM et al: Joint analysis of IVD herniation and degeneration by rat tail needle puncture model. *J Orthop Res*, 2017; 35: 258–68
- Showalter BL, Beckstein JC, Martin JT et al: Comparison of animal discs used in disc research to human lumbar disc: Torsion mechanics and collagen content. *Spine*, 2012; 37: E900–7
- Beckstein JC, Sen S, Schaer TP et al: Comparison of animal discs used in disc research to human lumbar disc: Axial compression mechanics and glycosaminoglycan content. *Spine*, 2008; 33: E166–73
- O'Connell GD, Vresilovic EJ, Elliott DM: Comparison of animals used in disc research to human lumbar disc geometry. *Spine*, 2007; 32(3): 328–33

## Conclusions

In the present study, we characterized the radiographical, histological, and biochemical features behind disc degeneration in the rat tail IVD, caused by puncture with 3 different sizes of needles at various time points. The size of the puncture needle affects the progression of the induced disc degeneration; larger needle size can cause more serious degenerative changes, and thus middle size (properly 21G) might be required to induce a proper degree IVDD at the proper time point. Our results suggest that the 2-week time point may be the best to use in further biological treatment studies.

## Conflicts of interest

None.

25. Elliott DM, Yerramalli CS, Beckstein JC et al: The effect of relative needle diameter in puncture and sham injection animal models of degeneration. *Spine*, 2008; 33: 588–96
26. Pfirrmann CW, Metzdorf A, Zanetti M et al: Magnetic resonance classification of lumbar intervertebral disc degeneration. *Spine*, 2001; 26: 1873–78
27. Lei T, Zhang Y, Zhou Q et al: A novel approach for the annulus needle puncture model of intervertebral disc degeneration in rabbits. *Am J Transl Res*, 2017; 9: 900–9
28. Norcross JP, Lester GE, Weinhold P et al: An *in vivo* model of degenerative disc disease. *J Orthop Res*, 2003; 21: 183–88
29. de Campos MF, de Oliveira CP, Neff CB et al: Studies of molecular changes in intervertebral disc degeneration in animal model. *Acta Ortop Bras*, 2016; 24: 16–21
30. Daly C, Ghosh P, Jenkin G et al: A review of animal models of intervertebral disc degeneration: pathophysiology, regeneration, and translation to the clinic. *Biomed Res Int*, 2016; 2016: 5952165
31. Issy AC, Castania V, Silveira JW et al: Does a small size needle puncture cause intervertebral disc changes? *Acta Cir Bras*, 2015; 30: 574–79
32. Jarman JP, Arpinar VE, Baruah D et al: Intervertebral disc height loss demonstrates the threshold of major pathological changes during degeneration. *Eur Spine J*, 2015; 24: 1944–50
33. Inoue H, Montgomery SR, Aghdasi B et al: The effect of bone morphogenetic protein-2 injection at different time points on intervertebral disk degeneration in a rat tail model. *J Spinal Disord Tech*, 2015; 28: E35–44
34. Richardson SM, Knowles R, Tyler J et al: Expression of glucose transporters GLUT-1, GLUT-3, GLUT-9 and HIF-1alpha in normal and degenerate human intervertebral disc. *Histochem Cell Biol*, 2008; 129: 503–11
35. Ha KY, Koh IJ, Kirpalani PA et al: The expression of hypoxia inducible factor-1alpha and apoptosis in herniated discs. *Spine*, 2006; 31: 1309–13
36. Li H, Liang CZ, Chen QX: Regulatory role of hypoxia inducible factor in the biological behavior of nucleus pulposus cells. *Yonsei Med J*, 2013; 54: 807–12